Finite element method analysis of propagation in a non magnetic coupled waveguide structure having α-power refractive index profile

Sanjeev Kumar Raghuwanshi* & Purnendu Shekhar Pandey

Department of Electronics Engineering, Indian Institute of Technology (Indian School of Mines), Dhanbad 826 004, India

The work presented in the paper is a numerical study of a waveguiding component. The structure studied is a coupler consisting of three closely-coupled weakly-guiding one-dimensional waveguides. The refractive index profile of the coupler has been allowed to vary arbitrarily. The scalar finite element method (FEM) has been used to separately extract the TE and TM modes supported by this coupler and propagate them along the structure using a beam propagation method (BPM). We excite structure with Eigen mode profile which can be well approximated by Gaussian shape pulse. The effect of waveguide separation has been well demonstrated by using an example. The Crank-Nicolson (CN) scheme has been used to stabilize the propagation and transparent boundary conditions (TBC) which have been used to absorb energy leaked by the waveguides to the outer boundaries. The work's main finding is that the coupling period of the structure can be changed by altering the index profile of the middle waveguide; step-, parabolic- and triangular-profile distributions have been studied and compared. In FEM analysis we have used the variable discretization step (δ) for the better accuracy of the results.

Keywords: Finite element method, Mode propagation method, Arbitrary refractive index profile

1 Introduction

Modecoupling phenomena and power exchange in a closely coupled waveguides have been the objects of several investigations in many years for the promising prospect of designing of optical switches and optical coupler to mention few[1-5]. Coupling between optical modes is an extremely essential in the design of integrated optical devices. Coupled mode theory well describes this energy exchange and serves as the primary tool for designing of optical couplers, switches and filters[6,7]. However, coupled theory cannot be applied when the refractive index profile of the waveguide is an arbitrary; this problem is the main target of this paper. In this paper we have analyzed three closely located waveguides having an arbitrary refractive index profile of a centre waveguide by using scalar finite element method approach. Here in entire analysis α controls the shape of refractive index profile of the middle waveguide. We have found that power coupling is the highest when the centre waveguide has a triangular refractive index profile ($\alpha = 1$). We can enhance the coupling between dissimilar waveguides by tuning the refractive index profile parameter "α" while the phase matching condition would satisfy. Finally we have

applied our mode propagation technique followed by Finite Element method approach to analyze the actual lowest order mode propagation to this structure. The coupling period of the power is compared and verified by mode propagation technique for the three cases like triangular refractive index profile case ($\alpha = 1$), parabolic refractive index profile case ($\alpha = 2$) and step index refractive index profile ($\alpha = 100$), respectively[8-22]. This study will be an extremely useful for the design engineer of optical switches, couplers, *etc*.

2 Finite Element Method Analyses for Coupled Waveguide Structure

In this section, the brief formulation of FEM is described while considering both TE and TM mode as an example in the coupled waveguide structure[4,5]. A planar waveguide is characterized by a permittivity profile which depends on one coordinate only, say x. If $\epsilon = \epsilon(x)$ is a varying function with x-coordinates we speak of an arbitrary index waveguide as shown in Fig. 1. We consider a nonmagnetic coupled waveguide structure having magnetic permeability $\mu = \mu_0$ (where μ_0 is free space permeability) throughout. Here a middle waveguide may consist of step index ($\alpha = 100$) permittivity profile too. The lowest is the substrate, on top of which there are one or

—————————
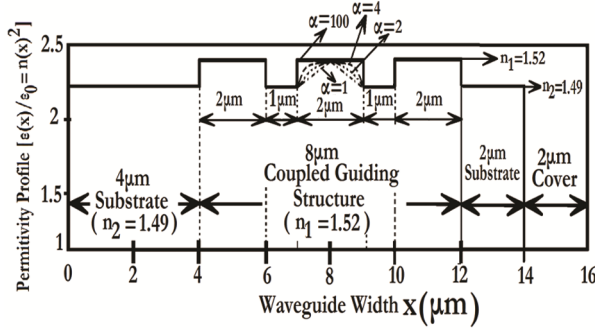Corresponding author (E-mail: sanjeevrus77@gmail.com)

Fig. 1 — Permittivity profile $\epsilon(x)$ versus cross section coordinate x for closely coupled waveguides.

many thin films, the topmost region is the cover. A coupled waveguide is characterized by a piecewise in-homogenous permittivity profile as shown in Fig. 1, the transverse region, $4 \leq x \leq 12$, which has a three coupled waveguide structure is denoted as the core and the refractive indices in the cover and the substrate are assumed to be constant. The waveguide separation for this closely coupled waveguide structure is 1 μm. The core of center waveguide obeys the α-power refractive index profile defined by:

$$n^2(x) = \begin{cases} n_s^2 (6 \leq x \leq 7) \\ n_1^2 - (n_1^2 - n_s^2) \, |x - 8|^\alpha , (7 \leq x \leq 9). \\ n_s^2 (9 \leq x \leq 10) \end{cases}$$

The waveguide separation for this closely coupled waveguide structure is 1 μm. The maximum refractive index in the core is n_1, and the refractive indices in the cover and the substrate are n_0 and n_s, respectively. Here we assume $n_s \geq n_0$. The various refractive index values taken for the present case is shown in Fig. 1.

The wave equation for the TE mode is given by[3-8]:

$$\frac{d^2 E_y}{dx^2} + \{k^2 n(x)^2 - \beta^2\} E_y = 0 , \qquad \ldots (1)$$

and for the TM mode [19];

$$\frac{d}{dx}\left(\frac{1}{n^2}\frac{dH_y}{dx}\right) + \left(k^2 - \frac{\beta^2}{n^2}\right) H_y = 0 , \qquad \ldots (2)$$

The boundary conditions require the continuity of E_y for TE mode is:

$$H_z = \frac{j}{\omega\mu_0}\frac{dE_y}{dx} \qquad \ldots (3)$$

and the boundary conditions require the continuity of H_y for TM mode is:

$$E_z = -\frac{j}{\omega\varepsilon_0 n^2}\frac{dH_y}{dx} \qquad \ldots (4)$$

at various interfaces. Before transforming the wave Eq. (1) and boundary conditions (Eq. (3) and Eq. (4)) into the variational problem, the parameters are normalized as:

$$\rho = \frac{x}{a} , E_y(x) = R(\rho) , D = \frac{A}{a}. \qquad \ldots (5)$$

Here "A" is the boundary at various coupled waveguide interface. The wave equation and boundary condition are then rewritten for TE mode A:

$$\frac{d^2 R}{d\rho^2} + [v^2 q(\rho) - w^2]R = 0 , \qquad \ldots (6)$$

$R(\rho)$ and $\frac{dR(\rho)}{d\rho}$ are continuous at $\rho = 0$ and $\rho = D \cdot$ $\qquad \ldots (7)$

Here, normalized transverse wave-number w, normalized frequency v, and normalized refractive-index distribution $q(\rho)$ are defined by:

$$\left.\begin{aligned} w &= a\sqrt{\beta^2 - k^2 n_s^2} , \\ v &= ka\sqrt{n_1^2 - n_s^2} , \\ q(\rho) &= \frac{n(x)^2 - n_s^2}{n_1^2 - n_s^2} \end{aligned}\right\} \qquad \ldots (8)$$

where, k is the wave number and a is the width (which is a 8 μm for the present case) of coupled waveguide structure. The solution of the wave Eq. (6) under the constraints of the boundary condition Eq. (7) is obtained as the solution of the variational problem that satisfies the stationary condition of the functional.

$$I[R] = -\int_{-\infty}^{\infty}\left(\frac{dR}{d\rho}\right)^2 d\rho + \int_{-\infty}^{\infty}[v^2 q(\rho) - w^2]\,R^2 d\rho \qquad \ldots (9)$$

The Eigen value matrix elements for the TE and TM modes are expressed as[4,5]:

$$\left.\begin{aligned} c_{0,0} &= \eta_0 - (3q_0 + q_1)\eta_0\frac{v^2}{12}\delta^2 + \eta_0\frac{w^2}{3}\delta^2 + \eta_0 w_0\delta , \\ c_{i,i} &= \begin{bmatrix} (\eta_{i-1} + \eta_i) - \\ (q_{i-1}\eta_{i-1} + 3q_i\eta_{i-1} + 3q_i\eta_i + q_{i+1}\eta_i)\frac{v^2}{12}\delta^2 \end{bmatrix} + (\eta_{i-1} + \eta_i)\frac{w^2}{3}\delta^2 \\ &\qquad (i = 1 - (N-1)), \\ c_{i,i+1} &= c_{i+1,i} = -\eta_i - (q_i + q_{i+1})\eta_i\frac{v^2}{12}\delta^2 + \eta_i\delta^2 \, (i = 0 - (N-1)) \\ c_{N,N} &= \eta_{N-1} - (q_{N-1} + 3q_N)\eta_{N-1}\frac{v^2}{12}\delta^2 + \eta_{N-1}\frac{w^2}{3}\delta^2 + w\delta , \end{aligned}\right\}$$

$$\ldots (10)$$

where

$$\eta_i = \begin{cases} 1 \text{ TE mode} \\ \frac{n_s^2}{n^2(\rho_i)} \text{ TE mode} \end{cases} \qquad \ldots (11)$$

$$\eta_{s0} = \begin{cases} 1 \text{ TE mode} \\ \frac{n_s^2}{n_0^2} \text{ TE mode} \end{cases} \quad \dots (12)$$

For nontrival solutions expect for $R_0 = R_1 = \cdots = R_N = 0$, the determinant of the matrix C should be

$$\det(C) = 0 \quad \dots (13)$$

where the element of the matrix C is given by Eq. (10) and discretization step δ is given by $\delta = D/N$. Equation (13) is a dispersion equation (eigenvalue equation) for the TE/TM modes in coupled waveguide structure. When the refractive-index distribution $q(\rho)$ of the waveguide and the normalized frequency v are given, the propagation constant β (implicitly contained inw) is calculated from Eq. (10) and Eq. (13). We have omitted the elaborated description on FEM, which can be accessed from our recently published papers[4,5].

3 Dispersion $(B - V)$ Characteristics of α- Power Coupled Waveguide Structure

Let us now calculate the guided modes of such coupled waveguide structure. We solve the mode Eq. (9) numerically by using finite element method. The effective permittivity $\epsilon_{eff} = \bar{\epsilon} = (\beta/k_0)^2$ stands for an Eigen value of the structure. When Eigen value β of matrix C of Eq. (13) is obtained, the corresponding Eigen vector $R_0, R_1, \dots \dots \dots R_N$ is calculated by the matrix operation. The solution of wave equation well converges for only few core divisions. Figures 2, 3 and 4 shows the allowed guided modes for $\alpha = 100, \alpha = 1$ and $\alpha = 4$ of the
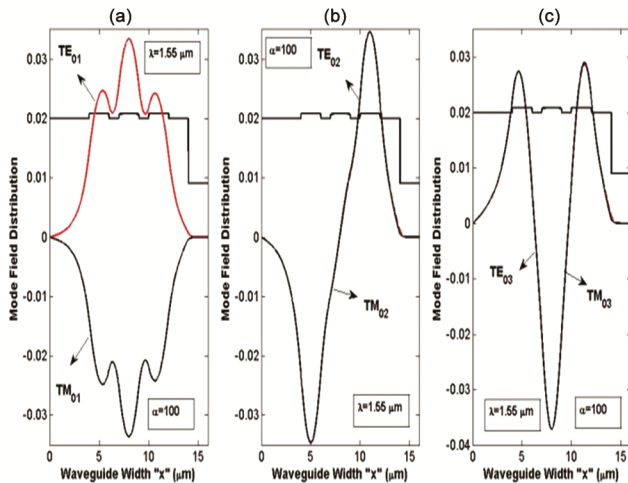
coupled waveguide structure, respectively, as revealed in Fig.1. Figure 2(a-c) reveals that for the case of step index refractive profile TE_{01}, TM_{01} modes are of an opposite mode field profile however other higher order modes have same field profile. These properties can be used to make a mode isolator and circulator. Figure 3(a-c) reveals that for the case of triangular refractive index profile $(\alpha = 1) TE_{01}, TM_{01}$ modes are in same mode field distribution however other higher order modes are in opposite mode field distribution. These properties can be used to make a polarizer, mode isolator, and rotator etc.

However Fig. 4 (a-c) reveals that for the case of parabolic refractive index profile $(\alpha = 4)$ all the modes are in an opposite mode field profile. Figures 5, 6 and 7 show the normalized propagation constant (b) versus V- number of coupled waveguide structure for the case of step index $(\alpha = 100)$, triangular index
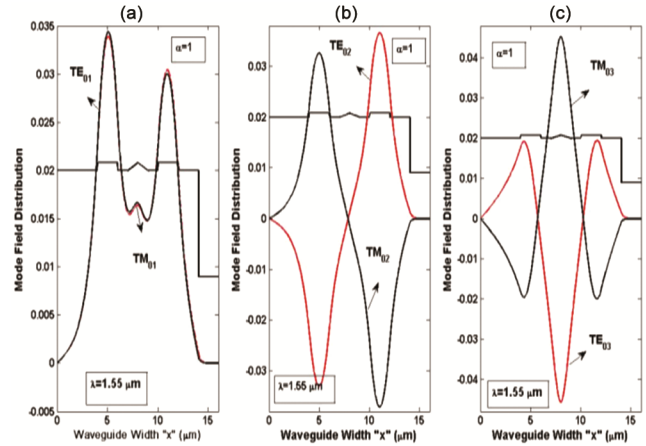

Fig. 3 — The waveguide structure Fig. 1 corresponds to $\alpha = 1$ carries first three guided TE and TM modes at $\lambda = 1.55 \ \mu m$.
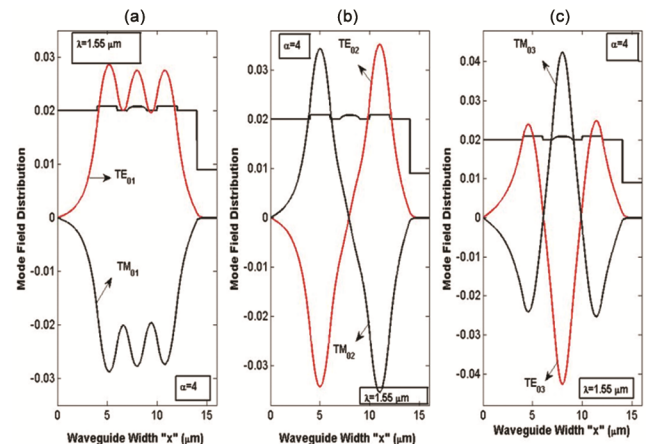

Fig. 4 — The waveguide structure Fig. 1 corresponds to $\alpha = 4$ carries first three guided TE and TM modes at $\lambda = 1.55 \ \mu m$.
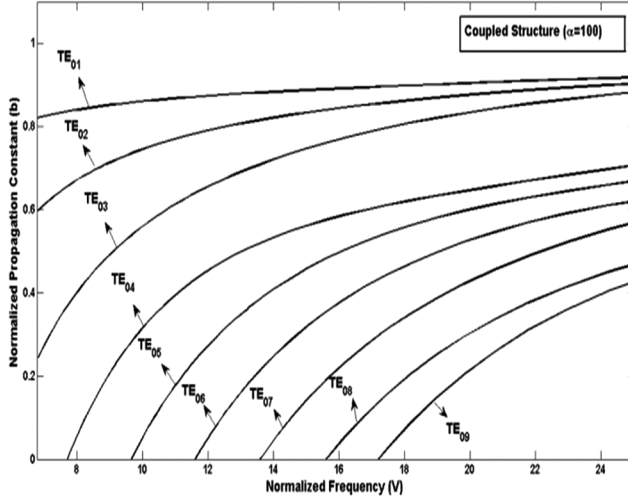

Fig. 2 — The waveguide structure as described in Fig. 1 corresponds to $\alpha = 100$ carries first three guided TE and TM modes at $\lambda = 1.55 \ \mu m$.

Fig. 5 — Normalized propagation constant (b) versus v- number (coupled waveguide width $a = 8\,\mu m$) of coupled waveguide structure corresponds to step index profile ($\alpha = 100$)case for TE mode case.
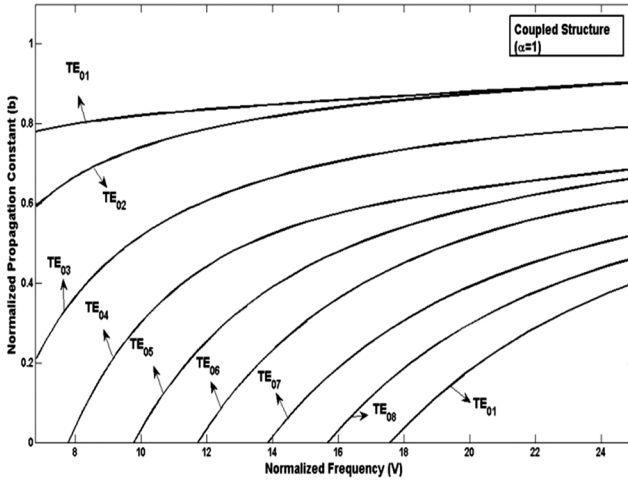

Fig. 6 — Normalized propagation constant (b) versus v- number (coupled waveguide width $a = 8\,\mu m$) of coupled waveguide structure corresponds to triangular refractive index profile ($\alpha = 1$) case for TE modes.

($\alpha = 1$) and parabolic refractive index ($\alpha = 4$) profile case, respectively.

4 Actual Mode Propagation by Mode Expansion Technique

If we introduce the scalar product of two functions as:

$$(g, f) = \int dx\, g^*(x), f(x) \qquad \dots (14)$$

One can easily show that the mode operator in Eq. (9) is hermitian. Therefore, its Eigen functions form a complete set of normalized and mutually
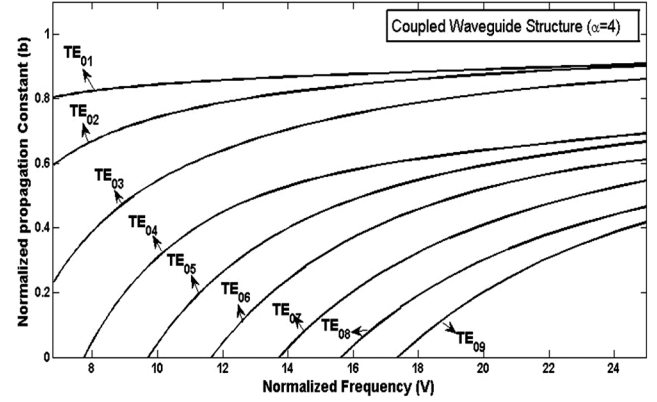

Fig. 7 — Normalized propagation constant (b) versus v- number (coupled waveguide width $a = 8\,\mu m$) of coupled waveguide structure corresponds to parabolic refractive index profile ($\alpha = 4$)case for TE mode.

orthogonal functions. Any square integrable function $f = f(x)$ may be decomposed into mode field's $e_r = e_r(x)$, $i.e.$,

$$f(x) = c_r e_r(x) \qquad \dots (15)$$

and the expansion coefficient c_r are given by

$$c_r = (e_r, f) = \int dx\, e_r^*(x) f(x) \qquad \dots (16)$$

If we want to know how an electric field $E = E(x, z)$depends on the propagation coordinate z we just have to work out the expansion coefficient:

$$c_r = \int dx\, e_r^*(x) E(x, 0) \qquad \dots (17)$$

and write as follows from wave solution.

$$E(x, z) = \sum_r c_r e_r(x) e^{i\beta_r z} \qquad \dots (18)$$

The differential equation for propagating a field along z direction is of second order, and therefore, two initial conditions should be specified, not just one, namely$f(x) = E(x, z = 0)$. We have computed allowed value of wave propagation constant β for entire wavelength range by using finite element method and then ride the actual pulse at $z = 0$ by using the Eq. (17) onto the coupled waveguide structure. We have presented Gaussian field profile into modes with positive effective permittivity and into actual guided modes. It has been found while doing simulation that incident field can be well represented by some of modes with positive effective refractive index. In present case the overlap integral factor R between the incidents Gaussian beam $f$and its representation $g$by guided modes which is defined by $|(g, f)|^2 = R(g, g)(f, f)$turns out to be 0.8783. This is acceptable range as the Cauchy-Schwartz

inequality says $0 \leq R \leq 1$. Figure 8 shows a Gaussian beam for the case of parabolic refractive index profile case which is a representation of positive effective index mode and cannot be distinguished with the actual Gaussian beam. However the guided modes only apparently deviate from the Gaussian shape of beam. For an example Fig. 11 shows the field of Fig. 8 which is approximated by input Gaussian pulse launched at $x = 5\ \mu m$ which then propagates along the z-direction with its appropriate propagation constant. It has been shown a simple way to calculate the propagation of a launched beam in a coupled waveguide structure.

Here we decompose the input pulse into a set of modes and let each modes propagates with its allowed propagation constant. In Figs 9, 10 and 11, the real

and positive effective index is considered because then it can be better approximated by Gaussian shape in the form of pulse. However for more realistic case the actual mode profile is quite deviated from Gaussian shape as shown in Fig. 8. By our approximated model it is assumed that power is within the computational window. Due to this, power might be reflected back into computational window from the computational boundary. Figures 9, 10 and 11 obtained while applying the transparent boundary conditions at the computational window.

It is possible to see the coupling effect for long distance propagation in this coupled waveguide
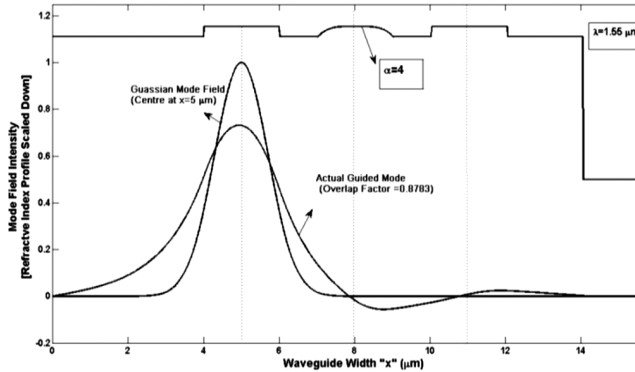

Fig. 8 — Actual guided modes have an effective index is greater than substrate refractive index and modes with positive effective index can be well approximated by Gaussian beam.
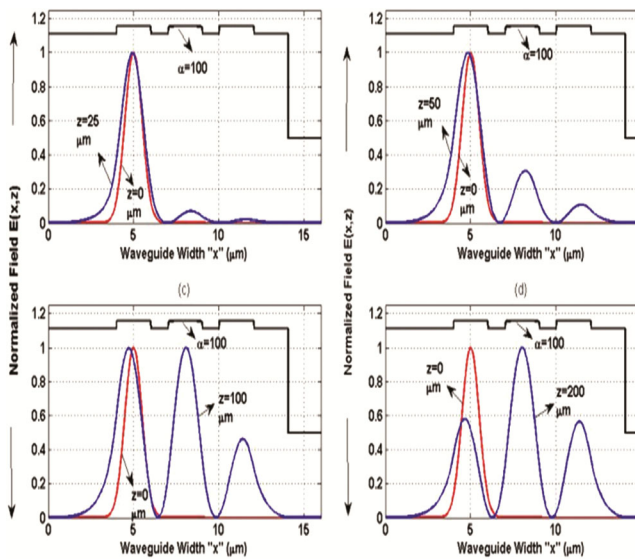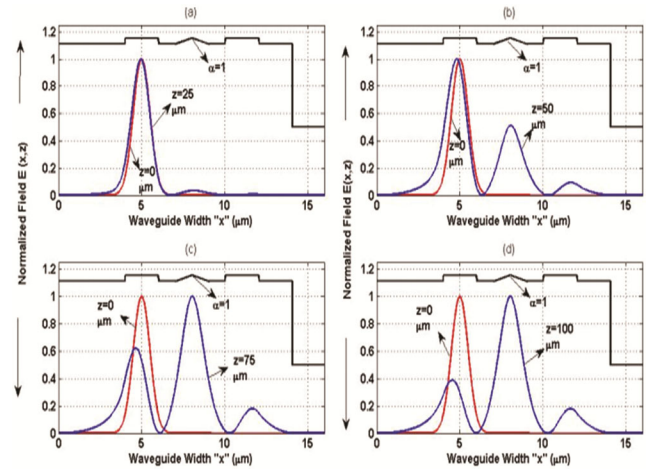

Fig. 10 — Simulated power coupling phenomena in a coupled waveguide structure having Gaussian pulse launched at $z = 0\ \mu m$, $x = 5\ \mu m$ corresponds to triangular index profile ($\alpha = 1$).

Fig. 9 — Simulated power coupling phenomena in a coupled waveguide structure having Gaussian pulse launched at $z = 0\ \mu m$, $x = 5\ \mu m$ corresponds to step index profile ($\alpha = 100$).
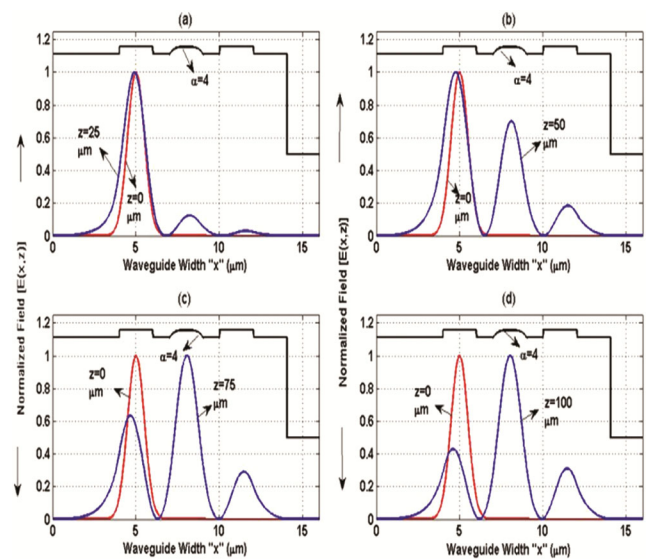

Fig. 11 — Simulated power coupling phenomena in a coupled waveguide structure having Gaussian pulse launched at $z = 0\ \mu m$, $x = 5\ \mu m$ corresponds to parabolic index profile ($\alpha = 4$).

structure. Figure 12 shows the effect of coupling phenomena for the case of $\alpha = 1$ and each guiding layer width is $1.5\,\mu m$. Power is periodically couple back and forth over the distance for the case of step index profile. We too compute the power in various layers of coupled waveguide structure over the distance of propagation, which is shown in Fig. 13. It is apparent that power has left the computational window which means that boundaries are transparent

indeed. The power in the computational window, after propagation by 1200 microns, is 0.7493 of the original power. As discussed before that the overlap of the incident beam with its representation by guided modes only was 0.7482. Everything in the incident field which is not a superposition of guided modes is radiated off. It is also apparent from Fig. 13 that power within the computation window converges to a limit. To compare the results with actual case we considered the case when the actual mode which is not perfectly Gaussian is launched into the coupled waveguide structure. Figure 14 shows the propagation behavior in this case. While comparing this figure with Fig. 12, it is apparent that close to beam injection at $z = 0$, the field pattern differs considerably. However, after a long distance of propagation, the Crank-Nicholson propagation scheme with Hadley's transparent boundary conditions[3] cannot be discerned from a mode propagation scheme. The incident beam field is decomposed into guided modes, and each guided mode propagates with its own propagation constant.

5 Results and Discussion

So far we have discussed the implication of propagation of a beam in a coupled waveguide structure with an arbitrary refractive index profile. The finite element method followed by mode expansion techniques used to compute the coupling period as shown in Figs 9, 10 and 11. It is possible to see the coupling effect for long distance propagation
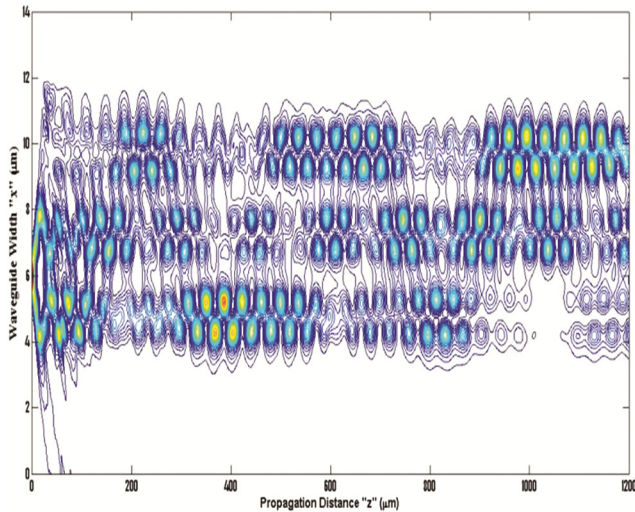

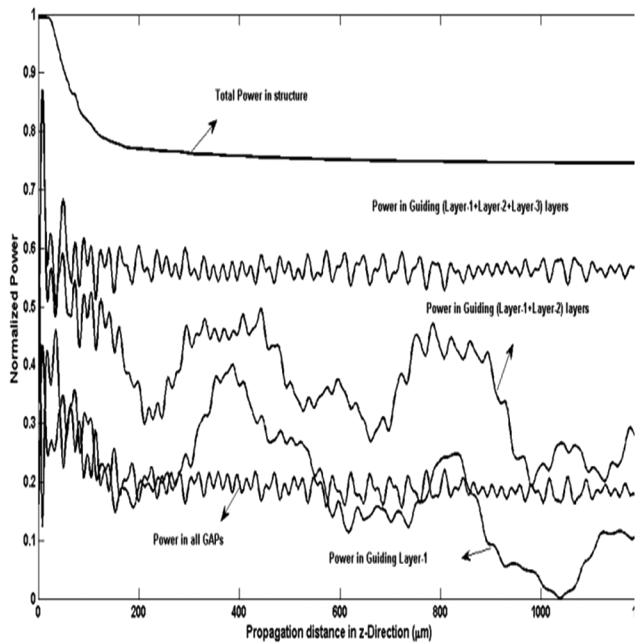Fig. 12 — Power coupling due to propagation in a coupled waveguide structure over a long distance.

Fig. 13 — Power variation along the direction of propagation. Power is shown in all the three guiding layers along with Gaps of coupled waveguide.
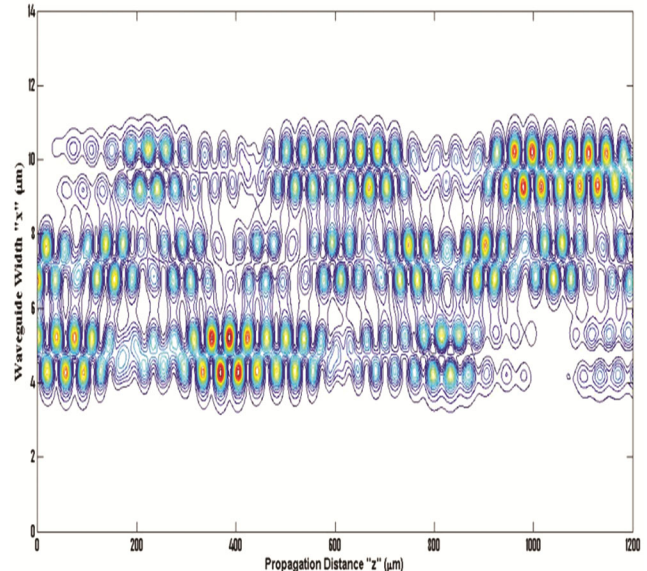

Fig. 14 — Actual Eigen mode, which propagates with its own propagation constant.

in this coupled waveguide structure. Figure 9 shows the effect of coupling phenomena for the case of step index profile. Power is periodically couple back and forth over the distance. We too compute the power in various layers of coupled waveguide structure over the distance of propagation. As discussed before that the overlap of the incident beam with its representation by guided modes only was 0.8783. Hence we choose to launch the input pulse as a Gaussian for all the cases at $z = 0\ \mu m, x = 5\ \mu m$. Figure 9(a) shows the field profile of the launched pulse at $z = 0\ \mu m, x = 5\ \mu m$ as well as after propagation up to $z = 25\ \mu m$ through step index profile coupled waveguide structure. Figure 9(b) corresponds to propagation up to $z = 50\ \mu m$ distance shows the power flowing to closely coupled structure. Figure 9(c) corresponds to propagation up to $z = 100\ \mu m$ distance shows the significant power transferred to centre waveguide ($\alpha = 100$), however the right most coupled structure could not fully captured the power from left most guided waveguide section. Figure 9(d) corresponds under steady state and propagation up to $z = 200\ \mu m$ shows that complete one cycle of propagation of power to both right most waveguide structure. Figure 10(a-d) shows the propagation behavior for the case of triangular refractive index profile ($\alpha = 1$) case. While comparing this figure with Fig. 9, it is apparent that cycle of power transfer is completed much early. Figure 10(b, c) shows that significant power is transferred up to $z = 75\ \mu m$ propagation distance and cycle is completed by $z = 100\ \mu m$ propagation length. In another case Fig. 11(a-d) shows the propagation behavior for the case of parabolic refractive index profile ($\alpha = 4$) case. In this case also the complete power transfer takes place early than step index profile case. Figure 11(a) shows the input pulse at $z = 0\ \mu m$ and $z = 25\ \mu m$. Figure 11(b, c, d) shows the condition of power transfer for $z = 50\ \mu m$, $z = 75\ \mu m$ and $z = 100\ \mu m$, respectively.

6 Conclusions

We present a mode coupling study in a kind of rare shape of three closely couple waveguide, showing physical analysis of mode profile and how the mode propagates in these waveguides. A few schemes for analyzing the physics are proposed and simulated. Results shown are mode profile, propagation constant, power coupling, *etc*. The guided modes of coupled waveguides can be very easily worked out

numerically. In fact, one calculates all modes and selects those with effective refractive index larger than cover index. An initial Gaussian beam, for example, can be well expanded into positive modes and the propagation as a sum of such modes seems very satisfactory, until the field hits the boundaries of the computational window. It is evident that it is reflected there which leads to unphysical interference phenomena. However, also the Crank-Nicholson scheme propagates with a unitary propagation operator such that the power within the computational window is conserved. Therefore we supplement the Crank-Nicholson scheme of propagation by transparent boundary conditions. At the boundary, we assume the field a plain wave with a definite wave number k. If it is an out-bound wave, nothing is done. If it is an inbound wave, we modify k such that it is neither outbound nor inbound. Thereby the field just outside the computational window may be predicted, so that we can safely calculate the second derivative at the boundary. Along distance propagation by the Crank-Nicholson scheme with transparent boundary conditions is presented. We have omitted the detail description of Crank-Nicholson scheme as it is widely discussed in numerous papers. We have proved that for the case of triangular refractive index profile case the power coupling is maximum, compared to step index profile case. Hence this study will be useful for engineers who are studying the techniques of optimization of optical coupler.

References

1   Franco M A R, Passaro A, Neto F S, Cardoso J R & Machado J M, IEEE Trans Magn*, 34 (1998) 2783.*

2   Boroujeni M A & Shahabadi M, J Opt A: Pure Appl Opt, 8 (2006) 1080.

3   Hadley G R, *Opt Lett*, 16 (1991) 624.

4   Raghuwanshi S K, Kumar S & Kumar A, *Optik*, 125 (2014) 5929.

5   Hardy A A, *IEEE J Quantum Electron*, 34 (1998) 1109.

6   Snyder A W, Chen Y & Ankiewicz A, *IEEE J Lightwave Technol*, 7 (1989) 1400.

7   Yasumoto K, *Opt Lett*, 18 (1993) 503.

8   S K Raghuwanshi & Rahman B M A, *Prog Electromagn Res-B*, MIT-USA, (2015).

9   Raghuwanshi S K & Rahman B M A, *IEEE Sens J*, (2015).

10   Raghuwanshi S K & Rahman B M A, *Opt Quantum Electron*, 2019 (under revision).

11   Marcuse D, *Theory of dielectric optical waveguides*, (Academic Press: New York), 1974.

12   Snyder A W & Love J D, *Optical waveguide theory*, (Chapman and Hall: London), 1983.

13 Zhang G D, He Y & Yang D, *Comput Math Appl*, 68 (2014) 770.

14 Obayya S S A, Rahman B M A & El-Mikati H A, *IEEE J Quantum Electron,* 36 (2000) 556.

15 Rajarajan M, Rahman B M A & Grattan K T V, *J Lightwave Technol*, 17 (1999) 243.

16 Rahman B M A, Wongcharoen T & Grattan K T V, *J Sci Soc Thailand*, 22 (1996) 43.

17 Katsriku F A, Rahman B M A & Grattan K T V, *J Lightwave Technol*, 14 (1996) 780.

18 Rahman B M A, Wongcharoen T & Grattan K T V, *J Sci Soc Thailand*, 21 (1995) 161.

19 Rahman B M A, Wongcharoen T & Grattan K T V, *Fiber Integr Opt*, 13 (1994) 331.

20 Raghuwanshi S K, Talabattula S & Selvarajan A, *J Indian Inst Sci,* 86 (2006) 667.

21 Raghuwanshi S K, Pattnaik P K, Talabattula S & Papannareddy R, *J Opt*, 35 (2006) 155.

22 Raghuwanshi S K, Pandey R R & Kumar V, *Int Nano Lett*, 1 (2011) 91.